3rd National Congress on Physical Sciences, 29 Sep. – 2 Oct. 2016, Sofia
Section: The Role of the Physical Sciences for the Bulgarian Industry and ...

Advances in Low-Temperature Liquid-Phase Epitaxy for Optoelectronic Devices Production

M. Milanova

Central Laboratory of Applied Physics, Bulgarian Academy of Sciences, 61 St. Petersburg blvd., 4000 Plovdiv, Bulgaria

Abstract. The low-temperature liquid-phase epitaxy (LPE) is the most simple, low cost and safe method for high quality optoelectronic devices fabrication. The crystallization process in the temperature range 400-600°C makes it possible to grow layers as thin as 1−10nm, as well as several microns thick, with a smooth surface and ?at interfaces. The high quality material in terms of lifetime, mobility and freedom from defects of the epitaxial layers derives from LPE growth under near equilibrium conditions.

Nevertheless, in recent years the use of LPE is limited especially for device fabrications, requiring large-area uniformity, new modes of liquid phase epitaxial growth remains the most important growth technique for a wide part of the new generation of optoelectronic devices, since the competing methods, molecular beam epitaxy MBE and metal-organic chemical vapor deposition MOCVD, are complicated and expensive although they offer a considerable degree of flexibility and growth controllability. This method well suited for growth and study of new materials and structures.

1 Introduction

Liquid-phase epitaxy (LPE) is an important technology and has been used in the production of III-V compound semiconductor optoelectronic devices for more than 50 years. Many semiconductor devices including light-emitting diodes (LEDs),laser diodes, infrared detectors, heterojunction bipolar transistors and heterointerface solar cells were fabricated at first with LPE. It allows to produce an excellent quality material, because the crystallization process in LPE is carried out at conditions not far from equilibrium and the cleansing action of the solution, by which impurities are retained in the liquid rather than being incorporated in grown crystal. For example, the internal efficiency of radiative recombination for a lightly doped direct-bandgap III-V binary compound and solid solutions grown by LPE is close to 100%, However, LPE is partially replaced nowadays with MBE and MOCVD. Majority of devices based on

multilayer QDs structures, superlattices, strained layer structures, and heterostructures with large lattice mismatch or heterostructures comprised of materials with substantial chemical dissimilarity (e.g. GaAs-on-silicon) are now produced using these techniques. A development of low-temperature variant of LPE widens its scope of applications in various novel structures and devices [1-6]. The lowering of the growth temperature provides the minimal growth rate values of 1–10 Å/s and makes it possible to obtain quantum well (QW) structures [7,8]. At the early stages of the process two-dimensional layer growth occurs, which provides structure planarity, precise layer composition and thickness controllability.

The choice of LPE depends on the needs and design of the epitaxial device structure. The growth of epitaxial structures with high layer thickness is difficult by MBE and MOCVD methods. The LPE process in the temperature range 600–400°C allows to grow multilayer structures containing layers with thicknesses of wide range: from few nanometers to several microns. Finally, because of its simplicity and low cost LPE is a suitable for growth and fundamental study of new materials and structures.

2 Low-Temperature LPE Growth of Ultrathin Layers

The success of the LPE method is strongly depend on the graphite boat design used for epitaxy growth. For the LPE growth of AlGaAs/GaAs layers and QW heterostructures "piston boat" technique has been used [9]. The substrate surface in this boat after the first wetting is always covered by a melt and this solves difficulties of wetting during the growth of AlGaAs heterostructures in the range 600–400°C. Piston boat design is shown in Figure 1. In this boat the melts of different compositions a placed in containers which can move along the boat body. The liquid phase falls down into the piston chamber and squeezes throw narrow slit into the substrate which allows mechanical cleaning of oxides films from

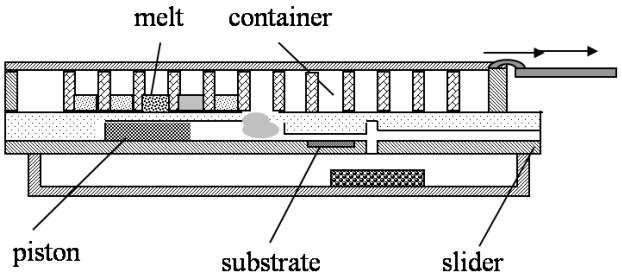

Figure 1: Design of "piston" boat for low- temperature LPE growth.

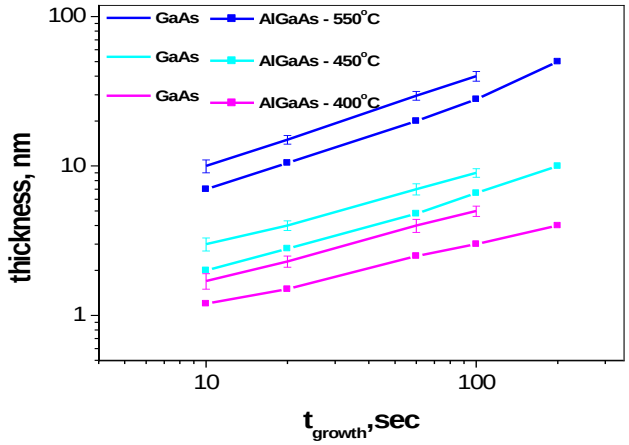

Figure 2: Dependence of GaAs and AlGaAs layer thickness on the growth time for different initial epitaxy temperature.

liquid phase and insures a good wetting. The crystallization is carried out from the melt 0.5–1 mm thick. After the growth of the layer liquid phase is removed from the substrate by squeezing of the next melt. The last liquid phase is swept from the surface by shifting the substrate holder out side the growth chamber.

Figure 2 shows the experimental dependencies of the GaAs and AlGaAs epitaxial layer thickness on the growth time for three initial epitaxy temperatures in the range of 600–400°C. The crystallization is carried out from a melt with thickness of 0.5 mm at a cooling rate of 0.5°C/min, supercooling of the melt 10°C. It shows that it is possible to fabricate AlGaAs heterostructures with layers as thin as 1–10 nm using the 10–20°C supersaturated melt for the crystallization time of 10 s.

The crystallization rate at the initial stage ($t < 100$ s) results in an elimination of the supersaturation condition provided by the initial supercooling of the melt. It can be seen that the crystallization rates of GaAs and AlGaAs layers at 550–400°C are of the same order of magnitude (0.1–1.0 nm/s) as in the MBE and MOCVD methods.

A necessary condition for optoelectronic devices performance is the optimum doping of the layers in the epitaxial structures. The experiments on doping using Te, Sn as n-type and Ge, Zn, Mg as p-type dopants covered a large range of carrier concentrations from 10^{16} to 10^{19} cm^{-3} for n-type GaAs and $Al_xGa_{1-x}As$ layers ($0 < x < 0.3$); from 5.10^{17} cm^{-3} to well above 10^{19} cm^{-3} for p-type $Al_xGa_{1-x}As$ layers ($0 < x < 0.3$), and from 10^{16} to 10^{18} cm^{-3} for n- and p-type $Al_xGa_{1-x}As$ layers ($0.5 < x < 0.9$) layers.

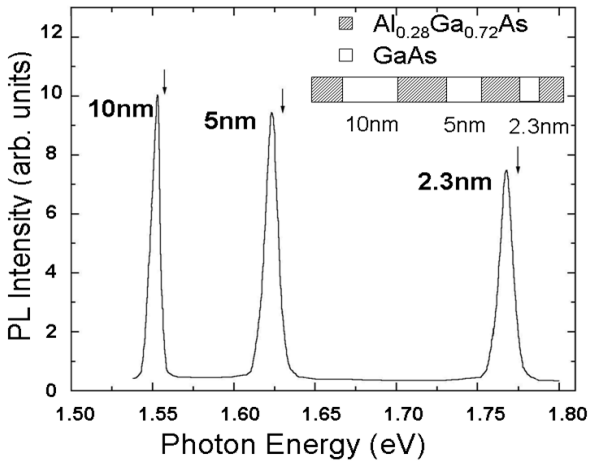

Figure 3: PL spectrum at 2 K of SQW AlGaAs/GaAs structure with 3 single quantum wells grown at 550°C, 500°C and 450°C.

Analysis of the spectral distribution of PL of the AlGaAs heterostructures with a narrow gap active region is a good way to demonstrate the planarity and crystal perfection of the grown structures. Figure 3. presents PL spectrum of AlGaAs/GaAs single quantum well (SQW) structure with three GaAs single quantum wells with different well width (2.3, 5 and 10 nm) grown at 550°C, 500°C and 450°C between thick $Al_{0.28}Ga_{0.72}As$ barriers, measured at 2 K. The arrows indicate the calculated energy values in the finite rectangular well at a temperature 2 K. From these calculations the emission peaks are assigned to the transition between $n = 1$ single-quantum-well electron and heavy hole states of the respective samples. The measured peak energy shifts by several meV below the calculated energy. A probable cause of this downshift of the emission energy is a 2D free exciton formation. The full width at half maximum values at 2 K are 4.5, 6.8 and 8.4 meV and they are comparable with those of MOCVD experiment. The average fluctuation in the well thickness over the interface caused by the island-like structure is smaller than two monolayers. This is an important result for the future progress in LPE fabrication of number QW electronic and optoelectronic devices.

3 AlGaAs/GaAs SQW Laser Diodes

QW lasers make it possible dramatically reduction of threshold current density because they require fewer electrons and holes to reach laser emitting compare to conventional double heterostructure lasers [10,11]. The lowest values of threshold current could be reached when the ma-

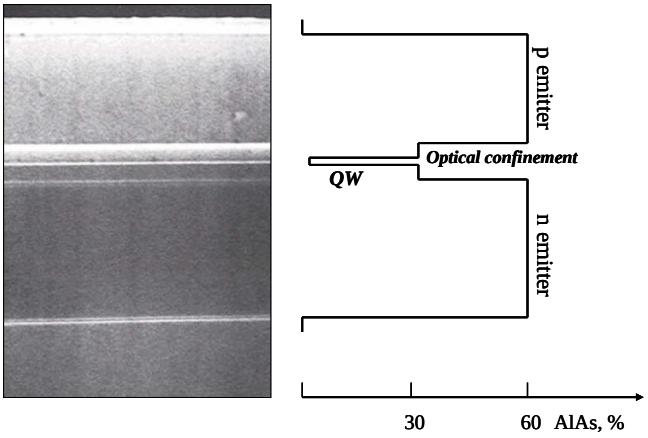

Figure 4: SEM cross section of SQW epitaxial laser AlGaAs/ GaAs structures and profile of AlAs distribution across the structure.

terials with the best luminescent properties are used. LT LPE allows reproducibly growth of uniform laser material with low threshold current density. SEM image of cross section of AlGaAs/ GaAs structures with SQW for fabrication separate confinement double heterostructure lasers is plotted in Figure 4. A 10 nm thick active layer of lower band-gap material (GaAs or $Al_xGa_{1-x}As$, $0.01 < x < 0.05$) is sandwiched between two cladding layers $Al_xGa_{1-x}As$ ($x \sim 0.3$), which ensure optical confinement of the laser light. N- and P-emitters are made from the material with smaller refractive indexes ($Al_xGa_{1-x}As$, $x \sim 0.6$). Heavy doped GaAs cap layers is grown on the surface in order to ensure a formation of low resistivity ohmic contacts.

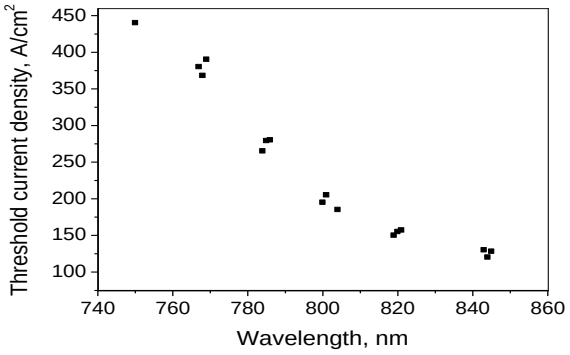

Figure 5: Dependence of the threshold current density on the emission wavelength.

The threshold current density j_{th} is measured on laser structures with wide stripe contacts for the different Fabry-Perot resonator length. The minimum value of the current density j_{th} of (120–150) A/cm^2 are measured for a cavity length L in the range 700–900 μm. The j_{th} values versus the wavelength λ of emitted light ($T = 300$ K, $L = 700$–900 μm) are plotted in Figure 5. for lasers with various AlAs contents in the active QW region with thickness d of 10 nm for λ values from 730 nm to 850 nm.

4 AlGaAs Photodiodes for Ionizing Radiation Detectors

Detectors designed for ionization measurements are used in two detection methods: one is an indirect detection method by which input radiation is converted into light by a scintillator and detected by photodiodes; the other is a direct detection method in which semiconductor detector directly detects a generated charge. These two types of detectors are selected and used according to radiation type and measurement applications.

The indirect detection method that is the combination of a photodiode with a scintillator is widely used in the detection and measurements of high energy electrons and gamma rays. Scintillators are available in various configurations to meet the users needs. In addition the performance of photodiodes can be freely modified to charge through ionization process. Si photodiodes are usually used for this purpose as a rule [12,13].

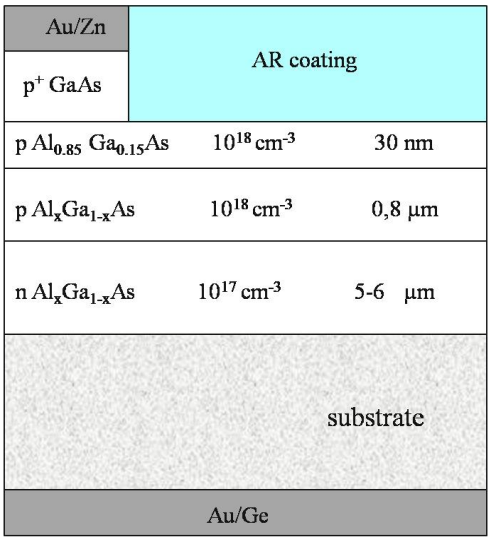

Figure 6: Schematic structure of p-n AlGaAs photodiode structure.

The application of the photodiodes on the base of AlGaAs/GaAs heterostructures makes it possible to improve the detector properties. In the first place this allows optimal matching of the luminescence spectrum of each type of crystal scintillator with the photosensitivity spectrum of the photodiodes by varying the band gap of the wide-gap window and of the photoactive region containing p–n junction. The large values of the band gap for the p–n junction material permit to decrease the dark current at room and higher temperatures, i.e., to ensure good threshold sensitivity and thermal stability of the detector.

To increase the band gap of the photoactive region a series of photodiodes on the base of (n–p)-$Al_xGa_{1-x}As$–p-$Al_{y>x}Ga_{1-y}As$–p^+GaAs heterostructures have been grown by low-temperature variant of the LPE method.

AlGaAs photodiodes with an area of 1 square cm have been made from the structures with different (0–30%) AlAs content in the p–n junction region. The cross-section of AlGaAs photodiodes is shown in Figure 6.

4.1 Spectral characteristics of AlGaAs photodiodes

Figure 7 shows the photoresponse spectra for the photodiodes. These spectra demonstrate that the increase of AlAs content in the photoactive region shifts the long-wavelength edge and the spectral position of the photosensitivity maximum toward higher photon energies in accordance with the change in the band gap of $Al_xGa_{1-x}As$. The high values

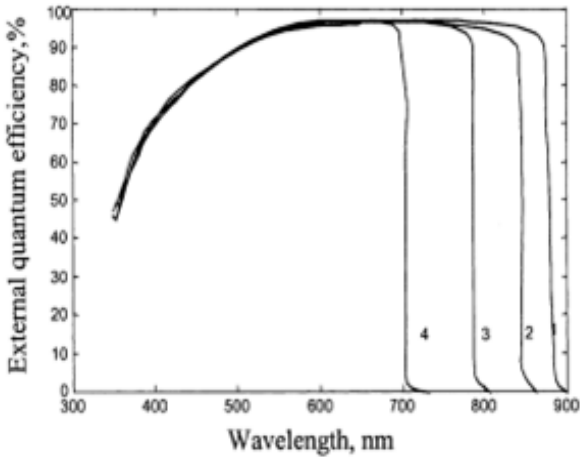

Figure 7: Spectral characteristics of AlGaAs photodiodes with different content of AlAs in photoactive region.

of the photocarrier collection efficiency at the maximum retain when the values of x varies in interval of 0–0.3 (curves 1–4). The photodiodes with spectral response 1 and 2 are effective to convert the red scintillator luminescence and those with spectral response shown by curves 3 and 4 are effective for conversion of luminescence light of $CdWO_4$, $Bi_4Ge_3O_{12}$ crystal scintillators.

4.2 Current–voltage characteristics of AlGaAs photodiodes

Fabricated p–n AlGaAs photodiodes are capable to operate in photovoltaic mode. This mode is used in most applications including spectral measurements of light and dose or exposure measurements of X-ray. The radiation induced photocurrent produced in photodiode is normally lower than 1 lA. The output current is directly measured from the detector by transimpedance amplifier (current mode). Leakage current or dark currents is the major source of signal offset and noise in diode applications operating in current mode. The "unbiased" diode is not actually operating at zero bias, but rather at a small positive or negative bias which is on the same order as the amplifier's offset voltage and which, in turn, introduces a finite dark current components. In Figure 8 are plotted the reverse branches of the dark current–voltage characteristics of the photodiodes with different AlAs content in the p–n junction region $x = 0$, 0.05, 0.15 and 0.3 (curves 1–4, respectively) obtained at room temperature. It is evident that major changes in the values of reverse current oc-

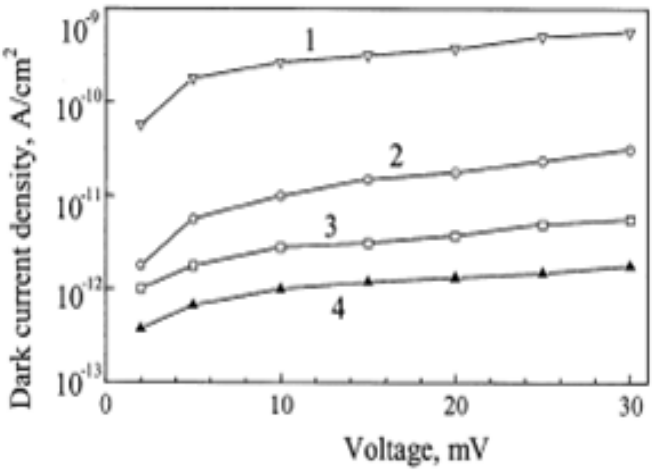

Figure 8: Current–voltage characteristics of AlGaAs photodiodes with different content of AlAs in photoactive region.

curred as a result of increasing the AlAs content in the AlxGa1_xAs near the p–n junction. We observed reduction in the reverse current value by two orders of magnitude with increasing of x down to values lower than 10^{-12} A/cm^2.

Shunt resistance (R_{sh}) is another means of defining the diode leakage and its impact on the related electronics. It is typical characteristic of the diode optimized for operation in photovoltaic mode. The shunt resistance is the dynamic resistance of the p–n junction at 10 mV bias voltage. For the developed photodiodes with AlAs content in thep–n junction region, R_{sh} is $\sim 10^{10}$ Ω. Since the leakage current is strong function of the temperature and increase with increasing the temperature, then so too must shunt resistant drops for the same temperature rise. His values retain sufficiently high up to 120°C (8–10 MΩ) which permits the operating of our photodiodes at these temperatures.

5 Single-Junction GaAs Solar Cells

For the first time a technology for high-efficiency solar cells based on AlGaAs/GaAs heterostructures is experimented in Bulgaria in the frame of the project 'Technology for solar cells based on III-V heterostructures', funded by the national priority program 'New technologies for power supply' [14]. The basic technological process is low-temperature liquid-phase epitaxy, developed at CLAP. The device processing established at CLSENES includes: layout of the devices, photolithography, selective metallization, surface passivation, and antireflective coating, and device characterization.

Sample structure. The investigated heterostructures for high-efficiency solar cell application contain 5 epitaxial films melt-grown on n-GaAs substrate: AlGaAs buffer layer, n-type GaAs layer as a base, p-type GaAs emitter, an ultrathin AlGaAs "window" layer , and a thin heavily doped p+GaAs contact layer. The latter forms a stable low-resistance contact to the p-side and protects the "window" layer during the production processes. As back surface field, the introduction of potential barrier at the back of the base improves the collection efficiency of the minority carriers generated in the photoactive region. This barrier is made by growing a n-type $Al_xGa_{1-x}As$ ($x \sim 0.2$–0.3) buffer layer on a GaAs substrate. The surface recombination on the front side of the solar cell is minimized by deposition an ultra-thin film (20–30 nm) "window" layer of wide band gap material $Al_{0.85}Ga_{0.15}As$ transparent to short-wavelength light.

The schematic and SEM cross-section of the epitaxial structure of the solar cell are shown in Figure 9.

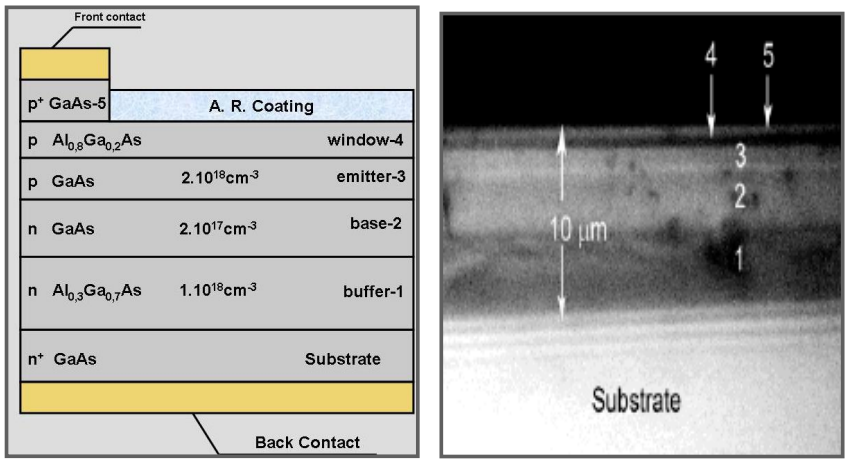

Figure 9: Schematic (left) and SEM (right) cross-section structure of single-junction GaAs solar cell.

5.1 Spectral characteristics of GaAs solar cell

The photoresponse spectra of the cells based on AlGaAs/GaAs heterostructures vary with the collection efficiency of carriers generated in n- and p-photoactive region and with the transmission spectrum of the wide band gap solid solution layer. The first factor determines the shape of the long-wavelength photosensitivity edge and the spectral variation of photoresponse, while the second factor determines the shape and position of the short-wavelength edge of photosensitivity. The external quantum efficiency of solar cells structure is displayed in Figure 10.

The short-wavelength edge of the photoresponse depends on the window solid solution composition and thickness. The AlAs content in the window layer is usually chosen in the range ($y \sim 0.8$–0.9). Maximum short-wavelength photoresponse values have been obtained for the cells with the wide band gap layer thickness of 30 nm. The high values of red spectral response are due to photon recycling process in solar cells which increases the upper limit of effective minority-carrier lifetimes for high quality epitaxial base material.

5.2 Photovoltaic characteristics of developed GaAs solar cells

Solar cells (2.5×2.5) mm^2 in size with a circle illumination area of 3.14 mm^2 are prepared. The width of the front metal lines is 8 μm, while the space (illuminated window) between the lines is 92 μm. The front

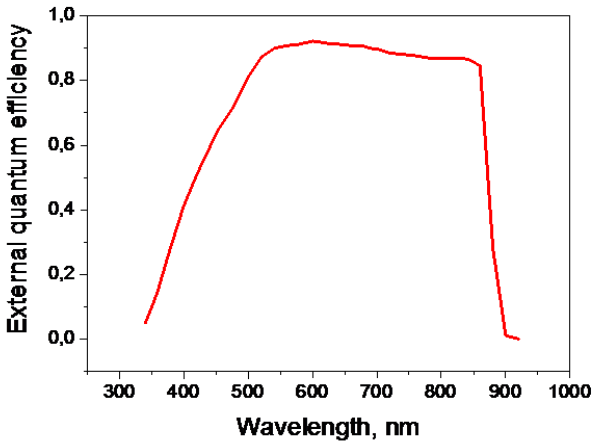

Figure 10: External quantum efficiency of GaAs solar cells.

and back metallization of the cell is Ni/Al system deposited by magnetron sputtering. A typical specific resistance of 5×10^{-5} Ohm.cm was achieved for n-type contact and higher than 10^{-4} Ohm.cm for p-type contact. A double layer anti-reflection coatingAl_2O_3/ZrO_2 is deposited on the front side of a AlGaAs/GaAs solar cell by the spin coating technique.

Figure 11 shows typical $I-V$ curve of the cells measured under standard test conditions AM 1.5.

The typical conversion efficiency obtained from GaAs cells under one-sun AM 1.5 global illumination is 18.7%. The corresponding open-circuit

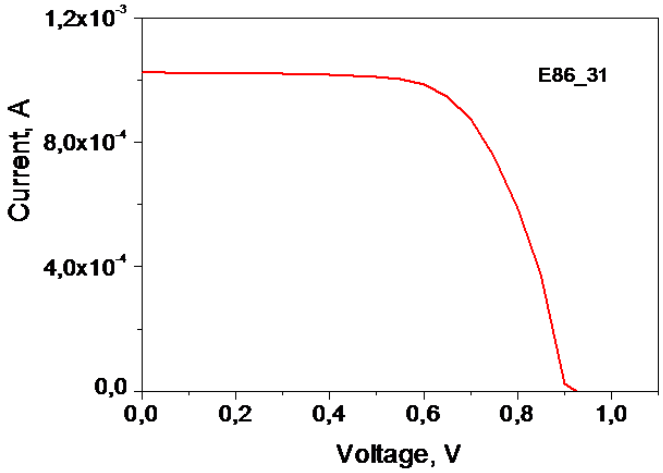

Figure 11: Typical $I-V$ curve for developed GaAs solar cell.

voltage Voc, short-circuit current density Jsc, and fill factor FF are 0.92 V, 29.87 mA/cm^2, and 68%, respectively. The best conversion efficiency of 19.5% for the developed cells under AM1.5 one sun conditions have been measured.

6 Summary

This paper demonstrates excellent capabilities of low-temperature LPE method for optoelectronic devices performance. Low threshold separate confinement double heterostructure lasers, high quantum efficiency photodiode for scintillation light detection and single-junction solar cells based on AlGaAs/GaAs heterostructures grown by LPE have been partially, or fully developed in Bulgaria.. The crystallization at low temperatures ensures the best structural and optical quality of the epitaxial multilayer grown structures containing both thick and ultrathin layers. The results indicate that the low-cost low-temperature LPE is suitable and promising growth method for new generation optoelectronic devices fabrication.

Bibliography

[1] A. Krier and X. L. Huang, Mid-infrared electroluminescence from InAsSb quantum dot light emitting diodes grown by liquid phase epitaxy (2002) *Physica E* **15** 159-161.

[2] D. Nohavica and J. Oswald, Preparation of periodic structures by meander type LPE (1995) J. Crys. Growth **146**, 287-290.

[3] A. Krier, S.E. Krier and Z. Labadi. Photoluminescence from InAs quantum wells grown by liquid-phase epitaxy (2000) *Appl. Phys. A* **71** 243-246.

[4] S. P. Guo, H. Ohno, A. D. Shen, Y. Ohno and F. Matsukura. Photoluminescence study of InAs quantum dots and quantum dashes grown on GaAs (211)B. (1998) *Jpn. J. Appl. Phys*. **37**, 1527-1530.

[5] V.N. Bessolov, S.G. Konnikov, M.V. Lebedev, K.Yu. Pogrebitskii and B.V. Tsarenkov, Experimental confirmation of model of relaxation liquid epitaxy with reversal of mass transport for making ultrathin III-V films (1990) *Sov. Phys. Tech. Phys*. **35** 99-101.

[6] A.T. Gorelenok, D.N. Rekhviashvili, M.Yu. Nadtochii and V.M. Ustinov, Two-dimensional electron gas in InGaAsP/InGaP heterostructures grown by liquid-phase epitaxy (1990) *Sov. Tech. Phys. Lett.* **16** 302-303.

[7] Zh.I. Alferov., V. M. Andreev, A.A.Vodnev, S.G. Konnikov, V.R Larionov., K.Yu. Pogrebitskii, V.D. Rymiantsev, V. P. Khvostikov, AlGaAs heterostructures with quantum-well layers, fabricated by low- temperature liquid-phase epitaxy (1986) *Sov. Tech. Phys. Lett*. **12** 450-451.

[8] M. Milanova, V. P. Khvostikov, Growth and doping of AlGaAs and GaAs layers by low-temperature liquid-phase epitaxy (2000) *J. Cryst. Growth* **219** 193-198.

[9] Zh.I. Alferov, V.M Andreev., S.G. Konnikov, V.R. Larionov, G.N. Shelovanova,. Investigation of a new LPE method of obtaining Al-Ga-As heterostructures, (1975) *Kristall Technik* **10** 103-105.

[10] Zh.I Alferov., V.M Andreev., A.Z. Mereutse, A.V. Syrbu, G.I. Suruchanu, V. P. Yakovlev, Super low threshold (Ith = 1.3 mA, T= 300 K) quantum-well AlGaAs lasers with uncoated mirrors prepared by liquid-phase epitaxy (1990) *Sov. Tech. Phys. Lett.* **16** 339-340.

[11] H. K. Choi, C. A. Wang, InGaAs/AlGaAs strained single quantum well diode lasers with extremely low threshold current density and high efficiency (1990) *Applied Physics Letters* **57** 321.

[12] O. Gilar, I. Pete, Combination of Si photodiode and a scintillator for a dose rate detector (1985) *Phys. Status Solidi a* **88** 375-380.

[13] J. H. Bai, J. H. Whang, The optimization of CsI(Tl)- pin photodiode for high-energy gamma ray detection (2011) *Progress in Nuclear Science and Technology*, **1**, 308-311.

[14] P. Vitanov, M. Milanova, E Goranova, Ch Dikov, Pl.Ivanov and V Bakardjieva, Solar cell technology based on III-V heterostructures (2010) *J. Physics:Conference Series* **253** 012044.